TÜBİTAK

Turk J Phys
36 (2012) , 197 – 205.

doi:10.3906/fiz-1107-7

# The influence of confinements on the photon flux spectra in amorphous silicon quantum dots

**Moafak Cadim ABDULRIDA[1], Nidhal Moosa ABDUL-AMEER[1] and Shatha Mohammad ABDUL-HAKEEM[2]**

[1] *Theoretical Nanoscience of Optoelectronic Devices Group, Department of Physics, College of Education (Ibn Al-Haitham), University of Baghdad, Adamiayh, Baghdad-IRAQ*
*e-mails: moafak@uobaghdad.edu.iq and moafak@uob.edu.iq*
[2] *Department of Physics, College of Science, University of Baghdad, Baghdad-IRAQ*

Received: 15.07.2011

**Abstract**

We have theoretically calculated the photon flux of radiative recombination in amorphous silicon quantum dots (a-SiQDs) at room temperature. These quantum dots have been ranged in their diameter 1 to 4 nm. The convolution of probability density function of deepest energy states of conduction $P_C(E)$ and valence $P_V(E)$ bands within the capture volume was adopted. The behavior of this function can be classified into four regions according to the quantum dot size. The effect of spatial and quantum confinements on the peak value of photon flux must be taken into account. We found that a blue shift is classified by the quantum confinement effect on the photon flux value, while a red shift appeared via the spatial confinement effect.

**Key Words:** Nanoscience, quantum dots, photon flux, quantum confinement

## 1. Introduction

The first observation of efficient and visible photoluminescence from silicon nanostructures, such as porous-Si [1] and crystalline Silicon (c-Si) quantum dots [2], was discovered in 1990.This is a remarkable discovery from a technological point of view because it opens the use of Si in light emitting devices compatible with Si-based optoelectronic integrated circuits [3]. The realization of silicon quantum dots (SiQDs) system has opened amazingly new area of physical research that deal with atomic scales. Active SiQDs have dimensions that are below ten nanometers [4, 5], and SiQDs systems are considered potential blocks for future nanoelectronics and nanophotonics [6]. In the process of searching for more efficient materials of lower dimension, it has been found that the amorphous silicon quantum dots, a-SiQDs, may be a convenient material for this purpose [7, 8]. In fact, this offers amorphous silicon two important advantages over crystalline silicon [9, 10]: firstly, the luminescence efficiency in a-Si is higher than in c-Si due to its structural disorder. Secondly, the band gap energy of a-Si QD is larger than that of c-Si (1.1 eV). Therefore a-Si is believed to be a good candidate for short wavelength light emitters [11].

However, since the transitions in silicon are almost indirect processes, direct transitions increase with reduced size of SiQDs [12]. The radiative transitions are associated with confined electron-hole pairs due to the mixing of wave functions [13]. The flood of photons that arise from the radiative recombination process is called the photon flux. In fact, the photon flux results from the convolution of the probability density function for each conduction and valence band. Using a simple model for radiative recombination in bulk amorphous silicon, the photon flux was first studied by Dunstan and Boulitrop [14]. Then, when this model was developed by Estes and Model [15, 16], for the case of a-Si nanostructures, the photon flux is calculated, which depends on the spatial confinement.

In this paper, we have calculated the photon flux in a new development that was proposed by Abdul-Ameer [17]. This new development considers the coexistence, in a-SiQDs, both spatial, and quantum confinement's effects. Also, we compare such photon flux with that in the case of only spatial confinement effect.

## 2. The model

The normalized luminescence photon flux spectrum, $P(hv)$, is the convolution of the probability density function of deepest energy conduction $P_C(E)$ and valence $P_V(E)$ band states within the capture volume [14–16]:

$$P\left(hv\right) = P_C\left(E\right) \circledast P_V\left(E\right) \equiv \int_{hv-\Delta E_V-E_g}^{\Delta E_C} P_C\left(E\right) P_V\left(hv - E_g - E\right) dE \tag{1}$$

It should be noted that the two $E$ values are in different reference frames [15]; and $E_g$ is the band gap energy of a-Si (1.6 eV). The probability density function for the conduction band is denoted by $P_{C(\text{lowest state})}(E)$, which gives the probability that the lowest-energy conduction band within the capture volume lies between $E$ and $E + dE$. It is then the probability that $n_C - 1$ states lie above the energy $E$ times the probability that $n_C^{th}$ state is between $E$ and $E+dE$, and is denoted by $P_{C[(n-1)states]}(E)$. Assuming these $n$ states are independent, $Pc\,(E)$ can be given as

$$P_C\left(E\right) = P_{C(\text{lowest state})}\left(E\right) P_{C[(n-1)\text{states}]}(E) \tag{2}$$

$$P_C\left(E\right) = V_C N_C\left(E\right) \left( \frac{\int_E^{\Delta E_C} N_C\left(E\right) dE}{\int_{-\infty}^{\Delta E_C} N_c dE} \right)^{n_C - 1} . \tag{3}$$

In the valence band, the probability, $P_{V(\text{highest state})}\left(E\right)$, obtains the probability of the highest-energy valence band state within the capture volume $V_C$, which lies between $E$ and $E+\mathrm{d}E$. While $P_{V[(n-1)\text{states}]}(E)$ is the probability that $n_V - 1$ states that lies below the energy $E$ times the probability that $n_V^{th}$ state is between $E$ and $E+\mathrm{d}E$. As in the conduction band, these $n$ states are assumed independent, therefore, $P_v(E)$ is written as:-

$$P_V\left(E\right) = P_{V(\text{highest state})}\left(E\right) P_{V[(n-1)\text{states}]}(E), \tag{4}$$

$$P_V\left(E\right) = V_C N_V\left(E\right) \left( \frac{\int_E^{\Delta E_V} N_V\left(E\right) dE}{\int_{-\infty}^{\Delta E_V} N_V dE} \right)^{n_V - 1} \tag{5}$$

where $N_C(E)$ and $N_V\ (E)$ are the conduction and valance band density of states respectively.

# 3. The results and discussion

## 3.1. Probability density function

As mentioned above, the probability densities function for either the conduction or the valence band results from the merger of two subordinate probabilities. The first is the probability of deepest state for each band, which increases with decreasing dot size. This means that the ratio of radiative transitions increases by considering this state, due to the increased number of radiatively recombined carriers. The other probability is: of $n-1$ states which decrease with decreasing dot size. This is related to the decreasing ratio of the radiative states and leads one to think that the ability of radiative recombination process is lower than that of the counterpart of the nonradiative recombination process. Figure 1 shows the probability density function for conduction and valence bands, respectively.

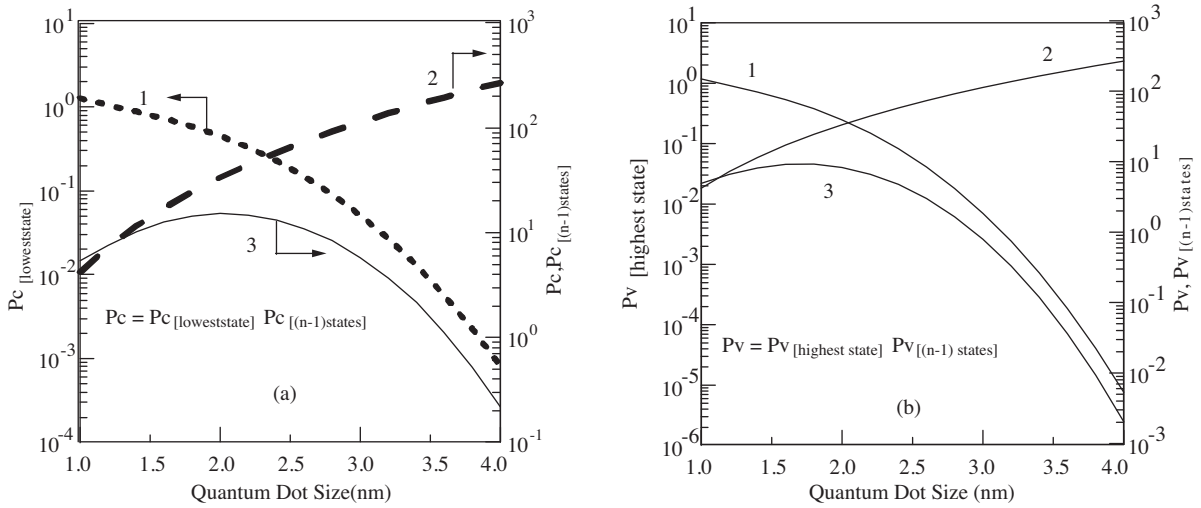


**Figure 1.** The curves 1 and 2 are subordinate probabilities density function, while curve 3 denotes the merger of the two probabilities for (a) the conduction band, and (b) the valence band.

When these two subordinate probabilities are merged in each band by multiplying, the effect of one on the aother appears. The effect can be classified into four regions. The first region, $R_t \geq 3.4$ nm, exhibits bulk-like behavior. The second region, 2.8 nm $\leq R_t \leq$ 3.4 nm, includes the large-dot sizes. The third region, 1.8 nm $\leq R_t \leq$ 2.8 nm, corresponds to the medium-dot sizes. Finally, the fourth region, 1 nm $\leq R_t \leq$ 1.8 nm, is related to the small-dot sizes. Each region exhibits behavior differing from each other.

Although the volume of the quantum dots in the first region is large, the ratio of the states, which contribute to the radiative recombination, is very low. In other words, the nonradiative states dominate because most transitions occur in only one band. Therefore, the total probability becomes very low, too. This behavior is similar to the bulk case where the radiative states contribution is very low.

In the second region, the total probability increases because the ratio of radiative states has increased with reduction in size. This is due to the transitions between the two bands.

In the third region, the values of the total probability are closing; they have reached maximum values. In this case, almost all the volume of the dots is exploited by the radiative states.

In the fourth region, it is very clear that the radiative states are dominated, but the volume of the dots has not a lot of states.

In fact, this analysis includes both the conduction and valence bands. Also, one can note, the probability density function in the valence band is higher than in the conduction band; and we think the reason for this is to keep the total allowed energy levels for transitions in the valence band greater than the number in the conduction band.

The convolution of these probabilities is a new function, which represents the photon flux. The principal factor of this function is the multiplication of the probability density function for conduction and valence bands. This factor, as indicated in Figure 2, has the same analysis as that of probability density function for conduction and valence bands, by taking in to account its rising value. If the photon flux is analyzed before the effect of probability density function, a difference will be found between the photon flux branch of conduction band and the photon flux branch of the valence band.

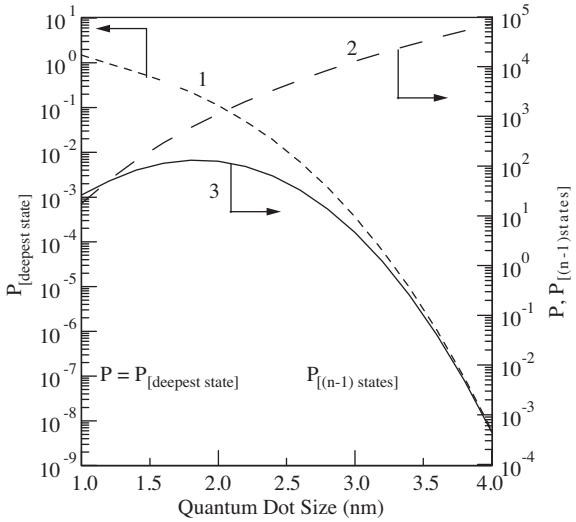


**Figure 2.** The curves 1 and 2 are subordinate probabilities density functions, while the curve 3 denotes the merger of the two probabilities for the conduction and valence bands.

## 3.2. Confinement effect on the photon flux

We turn now to the effect of the probability density function on the photon flux at each of the spatial and quantum confinements. With respect to each of the classified regions, photon flux has been plotted against photon energy. In fact, two sizes for each region have been computed to observe any size-dependent change in the photon flux. One can expect due to the spatial confinement that the difference in the wave number values $\Delta k$ becomes less than the corresponding value in bulk and may cause a transformation from indirect to direct gap structure. Therefore the lifetime of radiative recombination process rises above the lifetime of nonradiative recombination process. For this reason, the photon flux has a rise in its value. The effect of the quantum confinement, as mentioned previously, is to increase the band gap of a-SiQD [11]. In fact, the radiative recombination rate will increase as $\Delta k \to 0$. On the other hand, at small dimensions, the amorphous mode may disappear when the band gap has increased. For these reasons our model may exhibit similar behavior for direct material in the recombination process.

Starting with the first region (with 4 nm size), Figure 3 shows the spatial confinement effect, and Figure 4 shows the effect for quantum confinement. The photon fluxes after affecting the probability come down to a

very low value. This means that there are very few or no radiative states at this size. At 3.6 nm, the photon flux value appeared with a little rise. It can be said that the radiative recombination process is more active when the size is reduced in this region. In other words, a few transitions become radiative. It is also very clear, as seen in Figure 4, that the shifting in the energy, despite the photon flux, has the same behavior as the spatial confinement case.

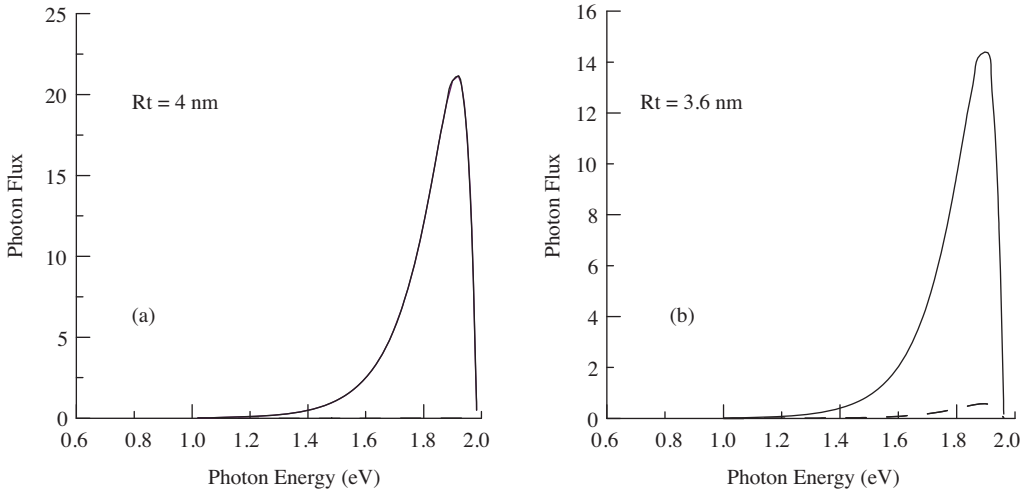


**Figure 3.** The photon flux for the bulk-like region under spatial confinement, showing the photon flux before (solid line) and after (dashed line) effect of the probability density function. Plot (a) is for 4 nm quantum dot size, and (b) for 3.6 nm quantum dot size.

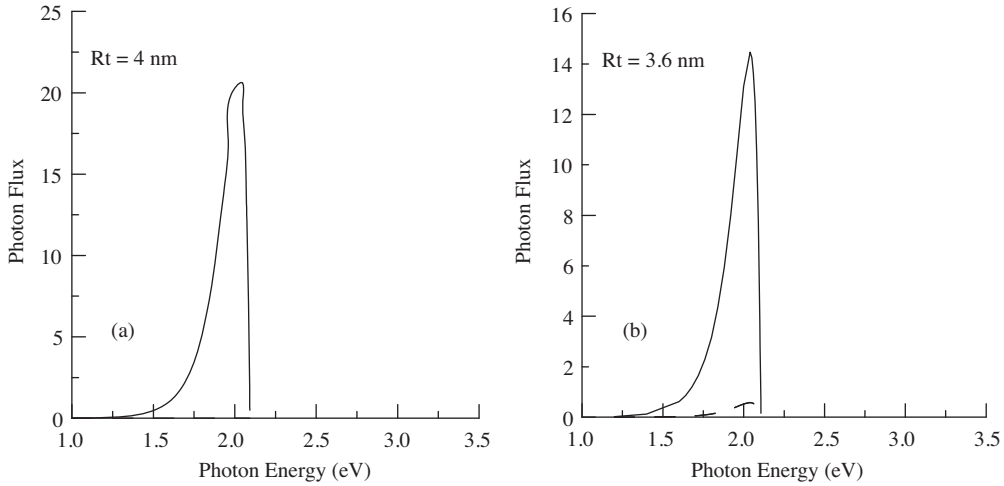


**Figure 4.** The photon flux for the bulk-like region under quantum confinement, showing the photon flux before (solid line) and after (dashed line) effect of the probability density function. Plot (a) is for 4 nm quantum dot size, and (b) is for 3.6 nm quantum dot size.

The effect of the probability can be noticed very clearly in a large-dot region. This is due to the increasing number of radiative transitions between the conduction and valence bands. One might think that, in addition to the delocalized transitions, the localized transitions are contributing to the radiative recombination process. In

fact, this explanation includes both the spatial and quantum confinements shown in Figures 5 and 6, respectively. Large jump in the photon flux can be observed by reducing the QD size in this region.

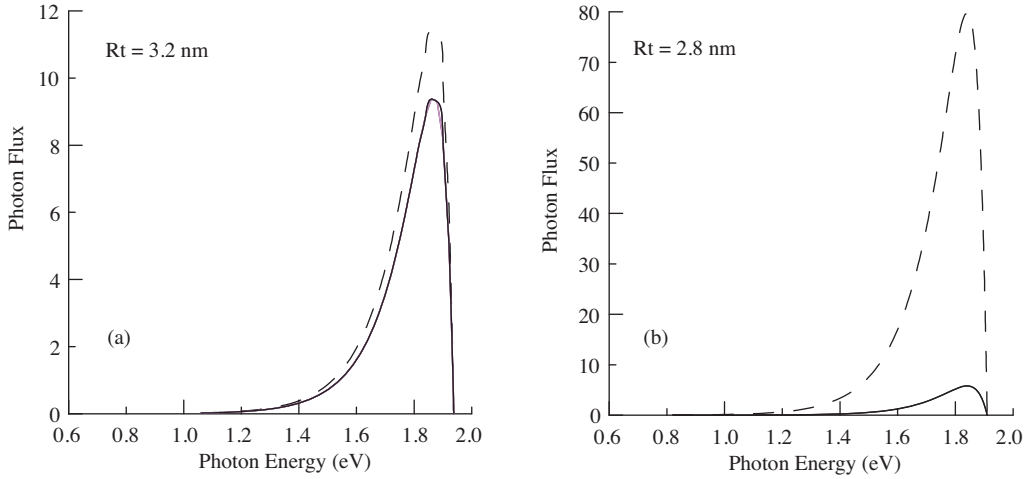


**Figure 5.** The photon flux for the large size region under spatial confinement, showing the photon flux before (solid line) and after (dashed line) effect of the probability density function. Plot (a) is for the3.2 nm quantum dot size and (b) is for 2.8 quantum dot nm size.

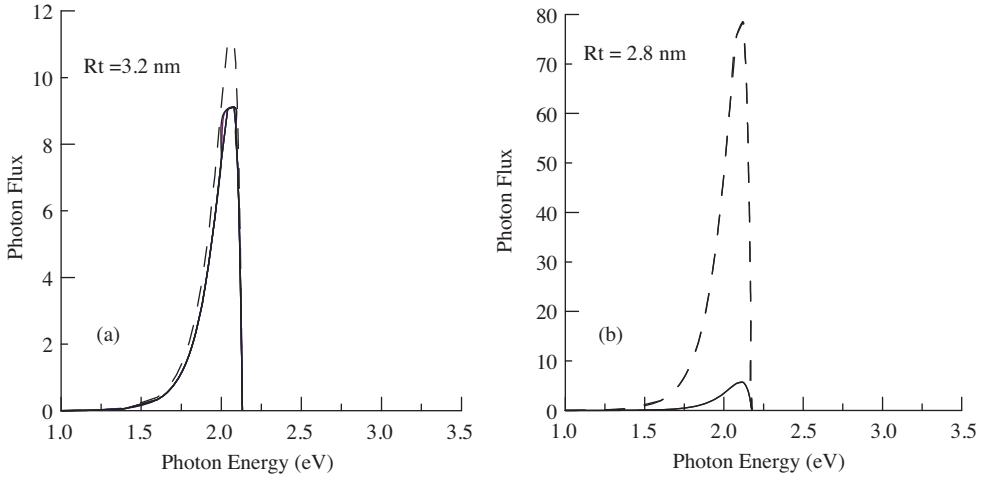


**Figure 6.** The photon flux for the large-size region under quantum confinement, showing photon flux before (solid line) and after (dashed line) effect of the probability density function. Plot (a) is for 3.2 nm quantum dot size, and (b) is for 2.8 nm quantum dot size.

The most important observation in Figures 7 and 8 is that the photon flux converges for all sizes in this region, which acts as a third region. Also, these values have reached maximum flux in this work. In fact, the decrease in nonradiative states at these dimensions is explained as that almost all the transitions are radiative in this region. It is expected from these calculations that a large number of carriers, having absorbed enough energy, are ready to recombine radiatively. Thus, most states at these sizes are radiative.

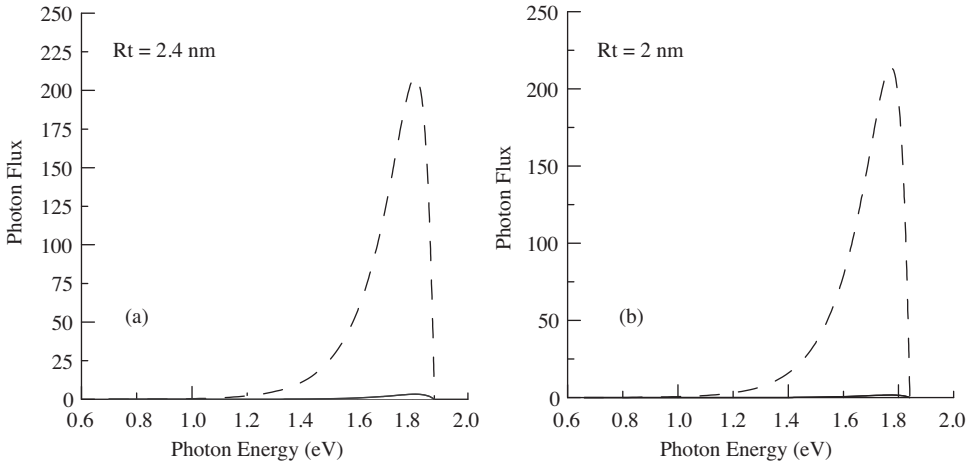


**Figure 7.** The photon flux for the medium-sized region under spatial confinement, showing the photon flux before (solid line) and after (dashed line) effect of the probability density function. Plot (a) is for 2.4 nm quantum dot size, and (b) is for 2 nm quantum dot size.

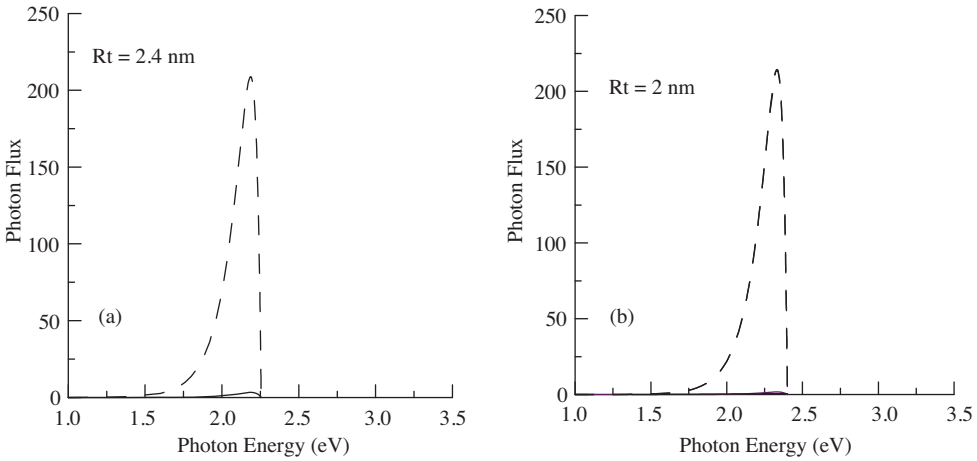


**Figure 8.** The photon flux for the medium-sized region under quantum confinement, showing the photon flux before (solid line) and after (dashed line) effect of the probability density function. Plot (a) for 2.4 nm quantum dot size, and (b) is for 2 nm quantum dot size.

The absorption energy for small QD sizes is rather small, resulting in reduced numbers of radiative transitions. This is illustrated in Figures 9 and 10, where the values of photon flux are seen decreasing with reduced size. This may lead one to think that the radiative recombination process is active but the number of transitions is low, by observing the magnitude of absorption energy.

In fact, both confinements contribute to shift the photoluminescence into the visible region where it can be tuned from red to blue by controlling sizes of the a-SiQDs. This tuning, which is known as blue shifting, is an outcome of quantum confinement. The red shifting is attributed to the spatial confinement only in a-SiQDs model. From this behavior and the high radiative quantum efficiency is the interpretation that the a-SiQDs material has been changed to a direct band gap material.

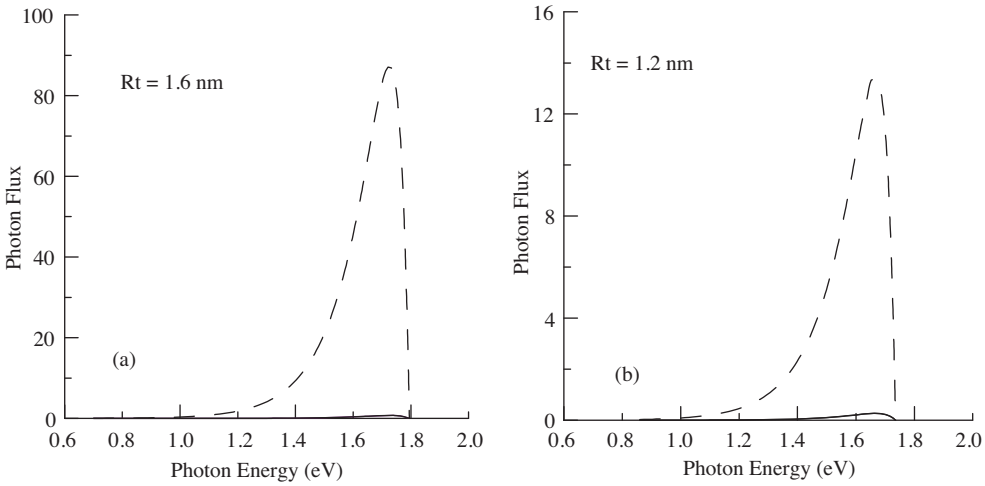


**Figure 9.** The photon flux for the small-size region under the spatial confinement showing the photon flux before (solid line) and after (dashed line) effect of the probability density function. Plot (a) is for 1.6 nm quantum dot size, and (b) is for 1.2 nm quantum dot size.

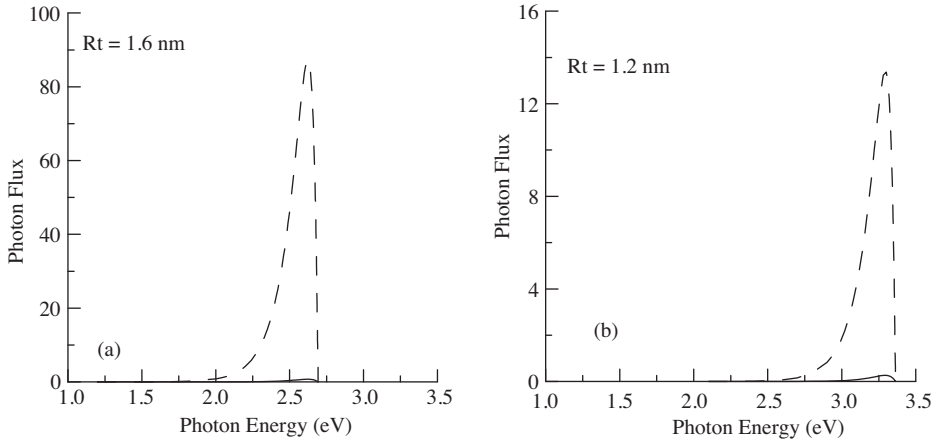


**Figure 10.** The photon flux for the small-size region under quantum confinement, showing the photon flux before (solid line) and after (dashed line) effect of the probability density function. Plot (a) is for 1.6 nm quantum dot size, and (b) is for 1.2 nm quantum dot size.

# 4. Conclusions

In this work we have tested our simulation for photon flux spectra. The effect of photon flux exhibits its behavior as photoluminescence intensity, where this behavior has only one shape style. This leads to the idea that the period of optical transitions associated with the various quantum dots sizes has the same mechanism. Also, the blue shifting appeared to be associated with spatial and quantum confinements, while the red shifting is shown associated with only the effect of spatial confinement.

## Acknowledgement

MCA and NMA acknowledge Prof. Dr. Abdl Jabbar A. Mukhlus, the Dean of College of Education (Ibn Al-Haitham), and Dr. Ahlam H. Jaffar Al- Mousawy for her useful and fruitful discussion.

## References

[1] L. T. Canham, *Appl. Phys. Lett.*, **57**, (1990), 1046.

[2] H. Takagi, H. Ogawa, Y. Yamazaki, A. Ishizaki, and T. Nakagiri, *Appl. Phys. Lett.*, **56**, (1990), 2379.

[3] F. Yonezawa, K. Nishio, J. Koga, T. Yamaguchi, *Journal of The Optoelectronics and Advanced Materials*, **4**, (2002), 569.

[4] J. S. Williams, R. G. Elliman, H. H. Tan, P. Lever, J. Wong- Leung, and C. Jagadish, *Materials Forum*, **26**, (2002), 74.

[5] C. J. Murphy and J. L. Coffer, *Focal Point*, **56**, (2002), 16A.

[6] I. Sychugov, R. Juhasz, A. Galeckas, J. Valenta, and J. Linnros, *Optical Materials*, **27**, (2005), 973.

[7] K. Nishio J. Koga, T. Yamaguchi, and F. Yonezawa, *Journal of Non-Crystalline Solids*, **312–314**, (2002), 323.

[8] K. Nishio J. Koga, T. Yamaguchi, and F. Yonezawa, *Phys. Rev. B*, **67**, (2003) 195304-1.

[9] H.-S. Kwach, Y. Sun, Y.-H. Cho, N.-M. Park, S.-J. Park, *Appl. Phys. Lett.*, **83**, (2003), 2901.

[10] N.-M. Park, T.- S. Kim, and S.-J Park, *Appl. Phys. Lett.*, **78**, (2001), 2575.

[11] N.-M. Park, C.-J. Choi, T.-Y. Seong, and S.-J. Park, *Phys. Rev. Lett.*, **86**, (2001), 1355.

[12] O. Bisi, S. U. Campisano, L. Pavesi and F. Priolo, "Proceedings of the International School of Physics (Enrico Fermi) Course CXLI Silicon Based Micro photonics: from Basics to Applications", Edited by O. Bisi, S.U. Campisano, L. Pavesi and F. Priolo, Amsterdam (1999), IOS Press, 47.

[13] T. Toyama, Y. Nakai, A. Asano, and H. Okamoto, *Journal of Non-Crystalline Solids*, **299–302**, (2002), 290.

[14] D. J. Dunstan and F. Boulitrop, *Phys. Rev. B*, **30**, (1984), 5945.

[15] M. J. Estes and G. Moddel, *Phys. Rev. B*, **54**, (1996), 14633.

[16] R. B. Wehrspohn, J-N. Chazalviel, F. Ozanam, and I. Solomon, *Eur. Phys. J. B*, **8**, (1999), 179.

[17] N. M. Abdul-Ameer, Ph.D. Thesis, University of Baghdad, College of Science, (2008).